Colorimetric High-Throughput Screening Assay to Engineer Fungal Peroxygenases for the Degradation of Thermoset Composite Epoxy Resins

Mikel Dolz[1], Ivan Mateljak[2], Daniel Méndez-Sánchez[1], Israel Sánchez-Moreno[1], Patricia Gomez de Santos[2], Javier Viña-Gonzalez[2]* and Miguel Alcalde[1]*

[1]Department of Biocatalysis, Institute of Catalysis, CSIC, Madrid, Spain, [2]EvoEnzyme S.L., Madrid, Spain

At present, the end-of-life management of thermoset composite epoxy resins is limited to incineration and landfill storage, highlighting the demand for the development of more sustainable measures. Due to their broad spectrum of C-H oxyfunctionalization reactions, fungal unspecific peroxygenases (UPOs) are becoming important biotechnological tools in organic synthesis while their potential use in biodegradation processes should not be underestimated. Here, we present a colorimetric screening assay aimed at engineering UPOs for the degradation of epoxy resins. We based our study on Hexflow® RTM-6, a commercial epoxy resin used extensively in the aeronautics sector. UPO mutants from the short and long families were initially benchmarked by GC/MS to determine their potential N-dealkylation activity on N,N-bis(2-hydroxypropyl)-p-toluidine (NNBT), the main structural scaffold of Hexflow® RTM-6. A reliable high-throughput colorimetric screening method was developed to quantify the lactaldehyde released by UPO attack on the tertiary amine of NNBT. Based on an evolved UPO from *Psathyrella aberdarensis* that was expressed by yeast, a small subset of mutant libraries with different mutational loadings was constructed and screened for NNBT N-dealkylation, thereby establishing a directed evolution platform as a vehicle to engineer UPO composite degrading variants.

Keywords: thermoset composites, epoxy resin, N-dealkylation, high-throughput screening, unspecific peroxygenase, directed evolution, *Saccharomyces cerevisiae*

INTRODUCTION

Thermoset composites are known for their exceptional mechanical properties, along with their thermal and chemical resistance. These materials are formed by combining a polymer matrix (usually a resin) with a reinforcing material like carbon or glass fiber (Pickering, 2006). Composites can be adapted to their final use by modifying the formulation of the mixture, such as the type and proportion of the resin and reinforcements, adapting them to a wide variety of applications including construction and aerospace (Zhang et al., 2021). An illustrative case is that of the epoxy resins used in the production of construction materials, in vehicle industries and as consumer goods like fiber-reinforced elements, adhesives, and coating and encapsulating materials (Acebo et al., 2017).

Thermoset plastics with appropriate properties are obtained when epoxy resins become cross-linked networks once they are cured. The resulting thermoset polymer can be produced with different chemical moieties, such as epoxides and tertiary amines. The resistance and complexity of

these materials makes their degradation and upcycling management a problem, with incineration and landfill storage as the main final destinations (Gharde and Kandasubramanian, 2019). As a consequence, over 306,000 tons of composite waste are accumulated each year around the world and large amounts of toxic substances are released through the thermal recycling of these materials that are harmful to the surrounding ecosystems. Not only has this issue been the subject of very little development but the use of these resins is far from decreasing, with their applications experiencing a constant growth over the last decade and expecting to increase further in the coming years (Sauer and Kuhnel, 2019).

In this context, and to avoid further damage to natural environments, green technologies are emerging to resolve the end-of-life issues associated with complex materials as part of Circular Economy approaches (Lucas et al., 2008; Moeser, 2014; Hou et al., 2016). As such, biotechnology can provide innovative solutions for the biodegradation of these complex plastics through the action of oxidative enzymes. Indeed, the natural activities of fungal oxidoreductases secreted by ligninolytic fungi make them particularly promising candidates to be used in novel degradation processes. These powerful oxidative biocatalysts are capable of degrading and depolymerizing structures as complex and recalcitrant as lignin (Alcalde, 2015). In particular, unspecific peroxygenases (UPOs, EC 1.11.2.1) constitute a unique superfamily of heme-thiolate peroxidases with mono(per)oxygenase activity triggered simply by H_2O_2, which serves as the final electron acceptor and main oxygen source. Phylogenetically sorted into two families (short- and long-UPOs), each with different substrate profiles and reactivities, UPOs stand-out as a compelling prospect for resin biodegradation. These enzymes can undertake a wide variety of one electron oxidation reactions and they carry an exclusive portfolio of C-H oxyfunctionalization chemistries that includes aromatic and aliphatic hydroxylations, alkene epoxidations, O-dealkylations, N-dealkylations, N-oxidations, sulfoxidations, deacylations and halide oxidations (Hofrichter and Ullrich, 2014). The N-dealkylations performed by UPOs are especially interesting, not least as a strong asset in the potential degradation of epoxy resins predominantly formed by chemical moieties based on tertiary amines.

In recent years, a wealth of UPO variants have been designed by directed evolution to be used in applications ranging from synthetic chemistry to bioremediation (Beltran-Nogal et al., 2022). In the current study, we have prepared a directed evolution platform for the engineering of future epoxy resin degrading UPOs. This platform includes a new robust colorimetric high-throughput screening (HTS) assay based on the detection of N,N-Bis(2-hydroxypropyl)-p-toluidine (NNBT), a representative scaffold of the commercial epoxy resin Hexflow® RTM-6. This assay is coupled to a yeast UPO expression system to readily construct and explore mutant libraries, aiding the future detection of improved UPO mutants for composite management.

MATERIAL AND METHODS

Strains and Chemicals
Hexflow® RTM-6 structure was provided by Aernnova Aerospace, S.A; NNBT was purchased from Toronto Research Chemicals (Toronto, Canada), Purpald reagent, Taq polymerase and Ceric Ammonium Molybdate Solution were purchased from Sigma (Madrid, Spain). Restriction enzymes BamHI and XhoI were purchased from New England BioLabs (Hertfordshire, United Kingdom). GeneMorph II mutazyme polymerase was purchased from Agilent (Santa Clara, CA, United States) The NucleoSpin plasmid kit, NucleoSpin gel and PCR clean-up kit were purchased from Macherey-Nagel (Düren, Germany). The episomal shuttle vector pJRoC30 was from the California Institute of Technology (Caltech) and protease-deficient S. cerevisiae strain BJ5465 (MATa ura3-52 trp1 leu2Δ1 his3Δ200 pep4::HIS3 prbΔ1.6R can 1 GAL) was obtained from LGC Prochem (Barcelona, Spain). Evolved UPO mutants PaDa-I, GroGu, and PabUPO-II were prepared as reported elsewhere (Molina-Espeja et al., 2014; Gomez de Santos et al., 2021). All chemicals were of reagent-grade purity.

Culture Media
Sterile minimal medium contained 100 ml 6.7% filtered yeast nitrogen base, 100 ml 19.2 g/L filtered yeast synthetic dropout medium supplement without uracil, 100 ml filtered 20% raffinose, 700 ml double-distilled water (ddH2O), and 1 ml 25 g/L filtered chloramphenicol. Synthetic complete (SC) dropout plates contained 100 ml 6.7% filtered yeast nitrogen base, 100 ml 19.2 g/L filtered yeast synthetic dropout medium supplement without uracil, 20 g autoclaved bacto agar, 100 ml 20% filtered glucose, 1 ml 25 g/L filtered chloramphenicol, and ddH2O to 1,000 ml. Sterile expression medium contained 500 ml autoclaved yeast peptone (YP) 2X, 67 ml 1 M filtered KH2PO4 (pH 6.0) buffer, 111 ml 20% filtered galactose, 22 ml filtered MgSO4 at 0.1 M, 31.6 ml absolute ethanol, 1 ml 25 g/L filtered chloramphenicol, and ddH2O to 1,000 ml. Yp medium 2X contained 20 g yeast extract, 40 g peptone, and ddH2O to 1,000 ml.

N-Dealkylation Reaction of NNBT by Unspecific Peroxygenase
Each reaction mixture contained 0.06 mg/ml purified enzyme, 5 mM NNBT, 2 mM H_2O_2 in 100 mM potassium phosphate buffer pH 6.0 (1 ml final volume). After incubating reactions at 30°C with 220 rpm in a Thermomixer for 2 h, samples were withdrawn and analysis by thin layer chromatography (TLC) and GC/MS.

Thin Layer Chromatography Analysis
TLC was used to initially monitor the oxidation reactions. Chromatograms were developed on silica gel plates (250 μm, Whatman, Maidstone, Kent, England) with acetonitrile 100% (v/v) as the solvent. The plates were dried before spots were revealed with a Ceric Ammonium Molybdate solution with H_2SO_4 ($CeH_{16}Mo_4N_4O_{16}$).

GC-MS Analysis

Reaction samples were mixed with an equal quantity of ethyl acetate and centrifuged at 11,000 RPM for 3 min. The organic phase was then pipetted out carefully, dried over $MgSO_4$ and analyzed by GC-MS with an GC-2010 Plus coupled to mass detector GCMS-QP2020ISQ (both from Shimazdu, Japan), equipped with a Rxi-5Sil MS column (30 m 9 0.25 mm I.D.). Helium was used as carrier gas at a flow rate of 1 ml/min and dodecane as internal standard. The column temperature was kept at 120°C for 1 min, then raised to 260°C at a rate of 20°C per min and kept for 6 min at such temperature. The ion source temperature was 300°C and the range of molecular weight was 20–400 m/z.

Mutant Library Construction

Seven independent mutant libraries were generated by error-prone PCR and further recombined *in vivo* by DNA shuffling. For error-prone PCR, *Taq* polymerase (*ep*PCR1) and GeneMorph II (*ep*PCR2) were used to achieve different mutational rates by varying the concentration of $MnCl_2$ and the amount of PCR cycles, respectively. The primers used for amplification were RMLN (5′-CCTCTATACTTTAACGTCAAGG-3′) and RMLC (5′-GGGAGG GCGTGAATGTAAGC-3′). The PCR mixture for *ep*PCR1 contained in a 50 μL final volume, dimethyl sulfoxide (DMSO) (3%), $MgCl_2$ (1.5 mM), deoxynucleotide triphosphates (dNTPs) (0.3 mM; 0.075 mM each), $MnCl_2$ (0.005, 0.010, 0.015, 0.10, 0.15 mM; depending on the desired mutational rate) *Taq* polymerase (0.05 U/μL), the template GroGu (10 ng) and RMLN and RMLC primers. The PCR mixture for *ep*PCR2 contained in a 50 μL final volume, dimethyl sulfoxide (3%), deoxynucleotide triphosphates (dNTPs) (0.08 mM; 0.2 mM each), GeneMorph II polymerase (0.05 U/μL), the template GroGu (56.12 ng/μL) and RMLN and RMLC primers. PCRs were carried out on a gradient thermocycler (MyCycler, Bio-Rad, United States) using the following parameters for *ep*PCR1 1: 95°C for 2 min (1 cycle); 95°C for 45 s, 50°C for 45 s, and 74°C for 1 min and 30 s (30 cycles); and 74°C for 10 min (1 cycle). The parameters for *ep*PCR2 were: 95°C for 2 min (1 cycle); 95°C for 30 s, 50°C for 30 s, and 72°C for 1 min and 30 s (20 and 30 cycles, depending on the aimed mutational rate); and 72°C for 10 min. PCR products were loaded onto a preparative agarose gel and purified with the NucleoSpin gel and PCR cleanup kit. The recovered DNA fragments were cloned under the control of the GAL1 promoter of the pJRoC30 expression shuttle vector, with the use of *BamH*I and *Xho*I to linearize the plasmid and to remove the parent gene. The linearized vector was loaded onto a preparative agarose gel and purified with the NucleoSpin gel and PCR cleanup kit. The corresponding PCR products (200 ng each) were mixed with the linearized plasmid (100 ng) and transformed into *S. cerevisiae* for *in vivo* gene reassembly and DNA shuffling. A total of 174 clones were evaluated in each library to determine the mutational landscape of each condition.

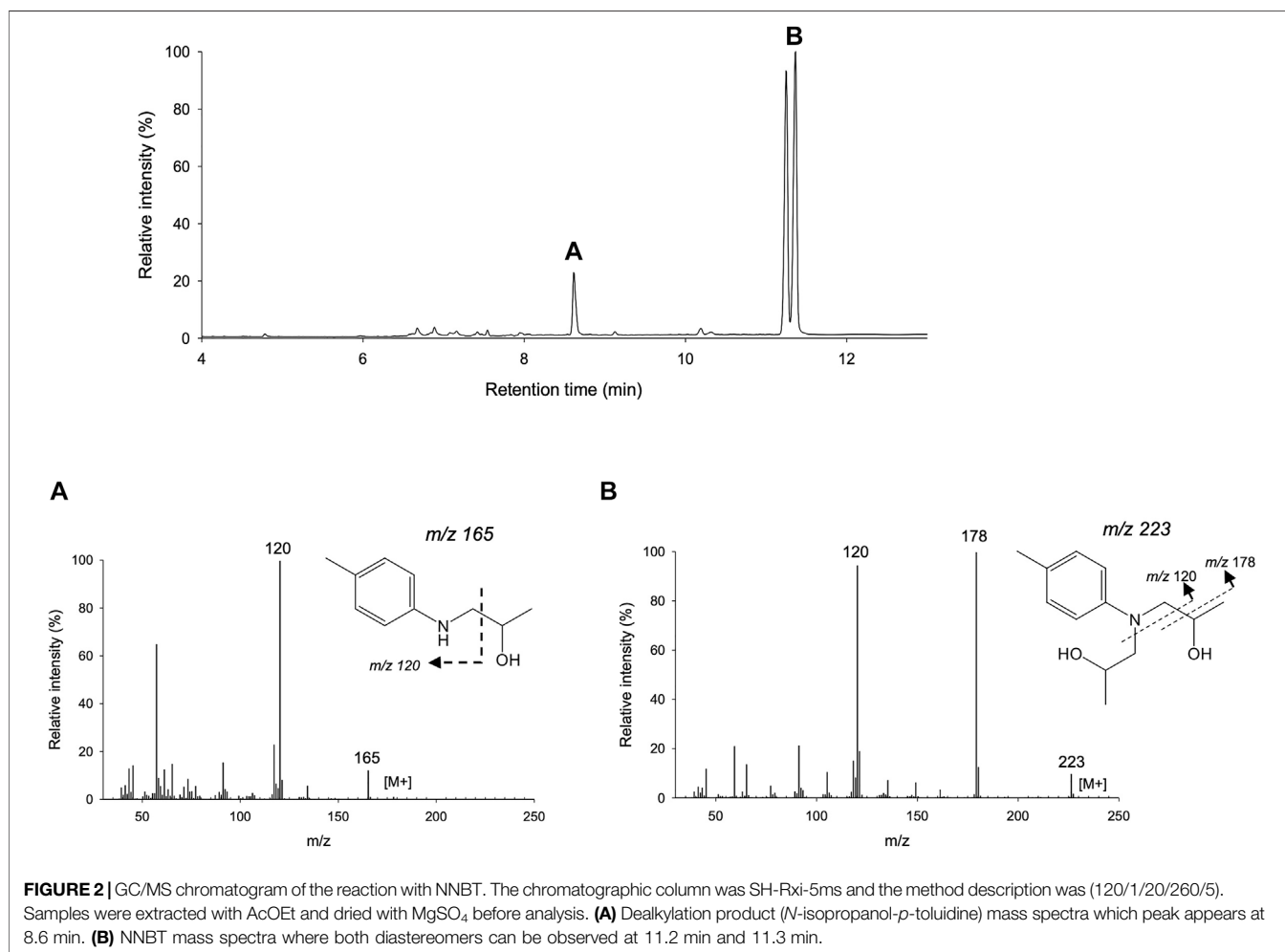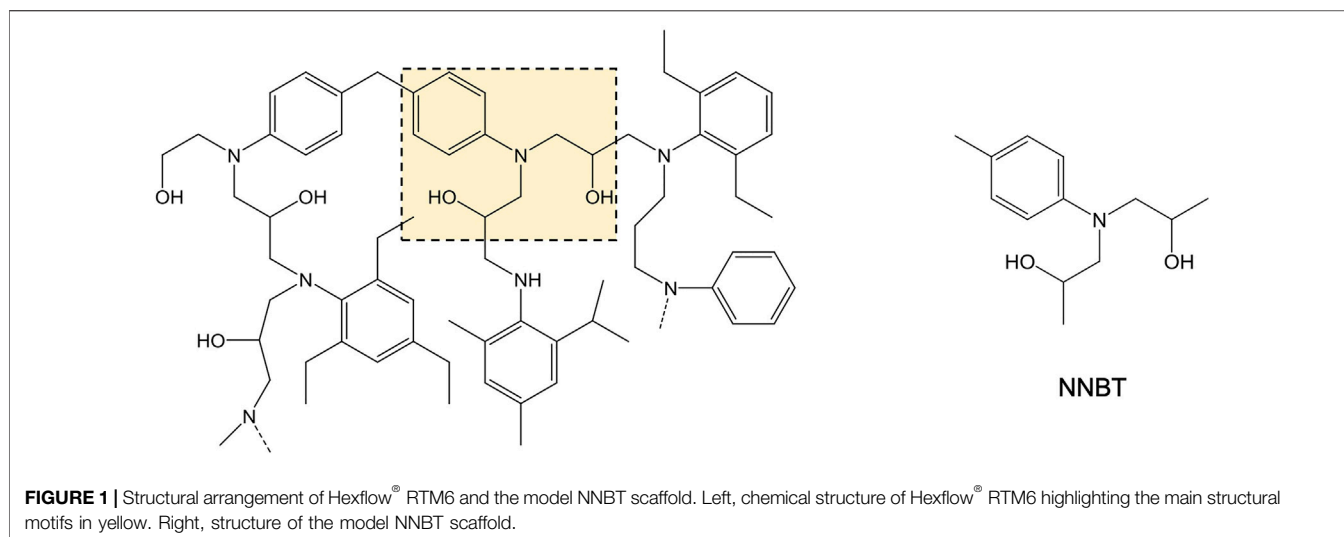## NNBT High-Throughput Screening Assay

Individual clones were picked and cultured in sterile half deep 96-well plates (CR1496c, EnzyScreen BV, Netherlands) containing 50 μL of minimal medium for well. In each plate, column 6 was inoculated with GroGu, and well H1 was inoculated with Aryl Alcohol oxidase (AAO). Plates were sealed to prevent evaporation and incubated at 30°C at 220 rpm with 80% relative humidity in a humidity shaker (Minitron-Infors, Biogen, Spain). After 48 h, 150 μL of expression medium was added to each well, followed by culture for an additional 48 h at 25°C. The plates were centrifuged at 2,500 rpm (at 4°C), and finally, 100 μL of supernatants were removed with the help of the liquid handler (Freedom Evoware 150 MCA, Tecan, Switzerland) and transferred to new standard 96 well plates (activity plate) where they were screened for activity with N,N-bis(2-hydroxypropyl)-*p*-toluidine (NNBT): 50 μL of NNBT reaction mix was added to each well of the activity plates and incubated for 5 min at 30°C and shaking (220 RPM). The NNBT reaction mix contained 15 μL of 1M KH_2PO_4 pH 6.0 buffer, 15 μL of 20 mM H_2O_2, 15 μL of NNBT (50 mM in acetonitrile) and 36.25 μL of ddH$_2$O. After 5 min incubation, 50 μL of Purpald Reagent (50 mM, dissolved in NaOH 2N) was added to each well and plates are vigorously shaken for 10 min. Finally, color development was recorded at 530 nm (SpectraMax ABS Plus, Molecular Devices, Sunnyvale, CA).
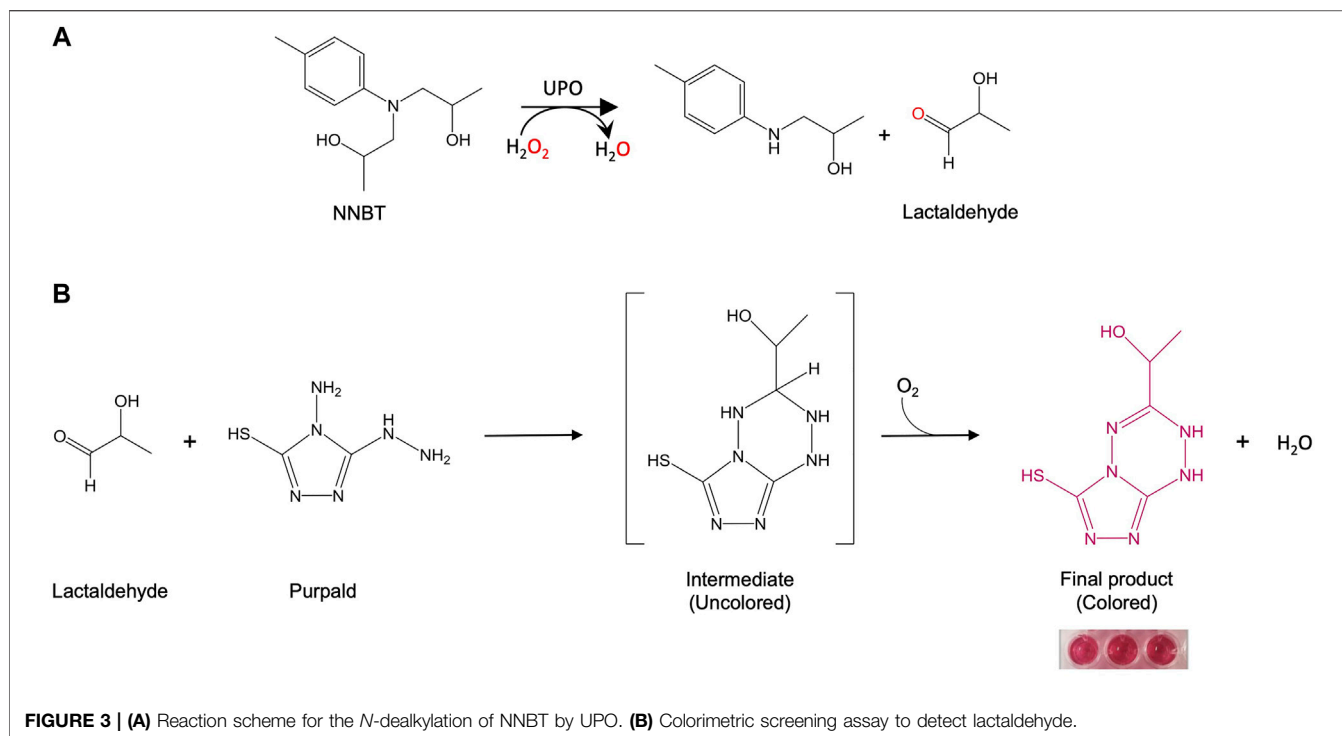
RESULTS AND DISCUSSION

In this study, Hexflow® RTM6 was selected as a representative epoxy resin as it is an aerospace qualified resin widely used as a thermoset composite. Indeed, in the aerospace industry this material is mainly employed as a matrix for Carbon Fiber Reinforced Polymer (CFRP) composites (Morelle et al., 2012; Greene, 2021). The Hexflow® RTM6 chemical structure is derived from the combination of an epoxide precursor with two di-amine hardeners, resulting in an amine-cured polymer (Morelle, 2015), **Figure 1**. Due to the inherent complexity and high hydrophobicity of the resin, it cannot be used as a substrate to develop a HTS assay for the directed enzyme evolution platform so rather, we analyzed the Hexflow® RTM6 structural arrangement to find a water-soluble scaffold that contains key resin motifs susceptible to enzymatic attack. After careful examination, N,N-bis(2-hydroxypropyl)-*p*-toluidine (NNBT) was chosen as a potential UPO substrate to design the HTS assay. NNBT carries a tertiary amine that may be crucial for the enzymatic depolymerization of the resin and since it appears in repeated moieties of the Hexflow® RTM6 backbone, its potential *N*-dealkylation by UPO could trigger resin cleavage and depolymerization.

UPO *N*-dealkylation activity has been reported for late-stage oxyfunctionalization reactions of pharmaceuticals but to date, it has never been tested with respect to the degradation of synthetic polymer scaffolds. As such, we benchmarked representatives of both UPO families (short- and long-UPOs), all of which can be produced recombinantly at high titers in *Saccharomyces cerevisiae* and *Pichia pastoris* after their *in vitro* evolution toward secretion (unpublished data and see

FIGURE 1 | Structural arrangement of Hexflow® RTM6 and the model NNBT scaffold. Left, chemical structure of Hexflow® RTM6 highlighting the main structural motifs in yellow. Right, structure of the model NNBT scaffold.

FIGURE 2 | GC/MS chromatogram of the reaction with NNBT. The chromatographic column was SH-Rxi-5ms and the method description was (120/1/20/260/5). Samples were extracted with AcOEt and dried with MgSO$_4$ before analysis. **(A)** Dealkylation product (N-isopropanol-p-toluidine) mass spectra which peak appears at 8.6 min. **(B)** NNBT mass spectra where both diastereomers can be observed at 11.2 min and 11.3 min.
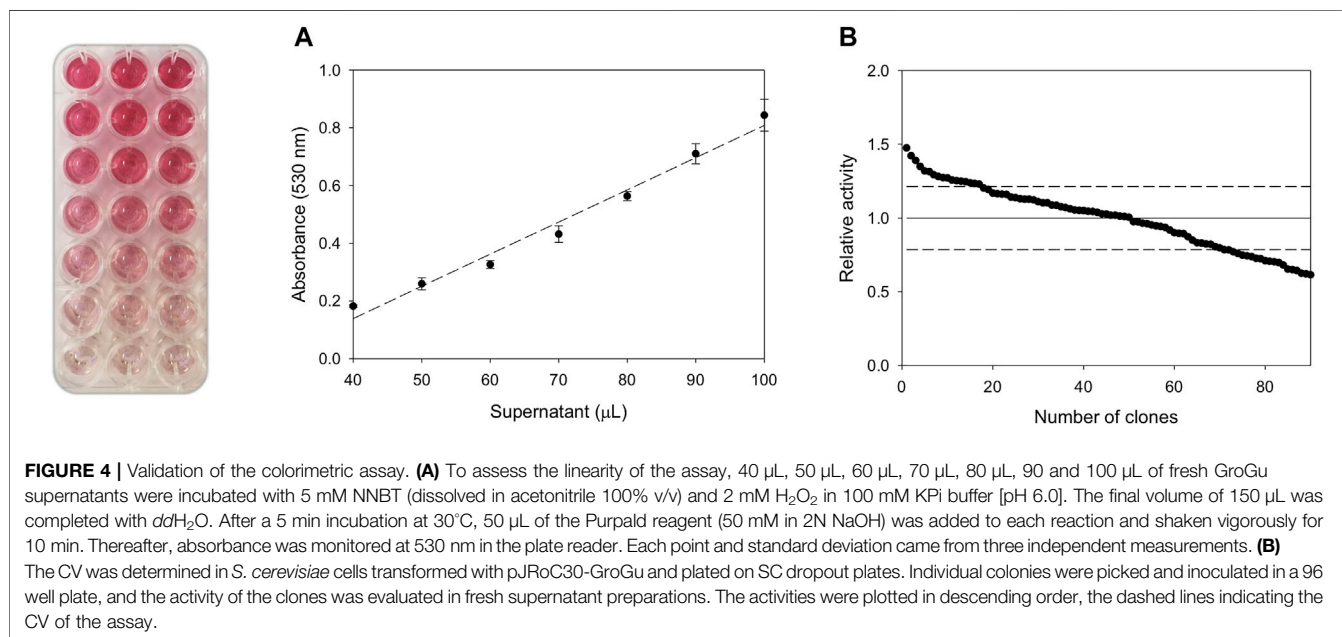
Molina-Espeja et al., 2014; Molina-Espeja et al., 2015; Gomez de Santos et al., 2021). This selection of UPO mutants included a set of long-UPOs (the PaDa-I variant, an evolved mutant of
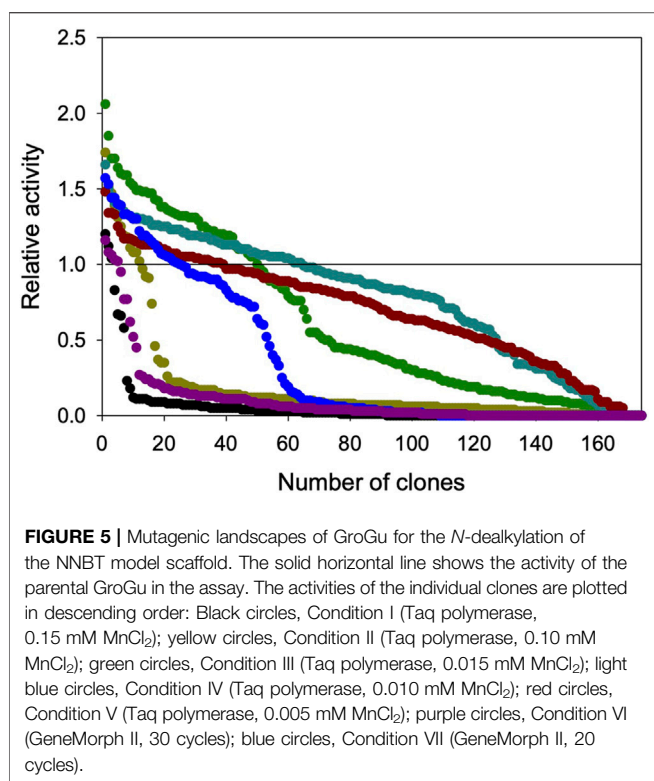
Agrocybe aegerita UPO - *Aae*UPO; the GroGu variant, an evolved mutant of *Psathyrella aberdarensis* UPO - *Pab*UPO-I; and the recombinant *Pab*UPO-II), as well as the

FIGURE 3 | (A) Reaction scheme for the *N*-dealkylation of NNBT by UPO. **(B)** Colorimetric screening assay to detect lactaldehyde.

recombinant short-UPO from *Marasmius rotula* (*Mro*UPO). After an initial assessment of the reaction by TLC, a clear spot appeared underneath the substrate staining for the reaction, especially with long-UPOs, indicating conversion of the colorimetric compound. This reaction was analyzed in detail by GC-MS, which confirmed the *N*-dealkylation of NNBT by UPO, with 12, 9, 8 and 4% conversion into the secondary amine by PaDa-I, GroGu, r*Mro*UPO and *Pab*UPO-II, respectively, **Figure 2**. All the UPOs tested are therefore candidates for directed evolution aimed at improving this *N*-dealkylation activity on NNBT, however, we opted to focus on the GroGu mutant given its high levels of production in a bioreactor (~0.3 g/L) and its versatility (acting over a wide range of pHs and temperatures, while

FIGURE 4 | Validation of the colorimetric assay. **(A)** To assess the linearity of the assay, 40 μL, 50 μL, 60 μL, 70 μL, 80 μL, 90 and 100 μL of fresh GroGu supernatants were incubated with 5 mM NNBT (dissolved in acetonitrile 100% v/v) and 2 mM H_2O_2 in 100 mM KPi buffer [pH 6.0]. The final volume of 150 μL was completed with *dd*H_2O. After a 5 min incubation at 30°C, 50 μL of the Purpald reagent (50 mM in 2N NaOH) was added to each reaction and shaken vigorously for 10 min. Thereafter, absorbance was monitored at 530 nm in the plate reader. Each point and standard deviation came from three independent measurements. **(B)** The CV was determined in *S. cerevisiae* cells transformed with pJRoC30-GroGu and plated on SC dropout plates. Individual colonies were picked and inoculated in a 96 well plate, and the activity of the clones was evaluated in fresh supernatant preparations. The activities were plotted in descending order, the dashed lines indicating the CV of the assay.

FIGURE 5 | Mutagenic landscapes of GroGu for the *N*-dealkylation of the NNBT model scaffold. The solid horizontal line shows the activity of the parental GroGu in the assay. The activities of the individual clones are plotted in descending order: Black circles, Condition I (Taq polymerase, 0.15 mM MnCl₂); yellow circles, Condition II (Taq polymerase, 0.10 mM MnCl₂); green circles, Condition III (Taq polymerase, 0.015 mM MnCl₂); light blue circles, Condition IV (Taq polymerase, 0.010 mM MnCl₂); red circles, Condition V (Taq polymerase, 0.005 mM MnCl₂); purple circles, Condition VI (GeneMorph II, 30 cycles); blue circles, Condition VII (GeneMorph II, 20 cycles).

containing an hybrid catalytic active site among long-UPOs (Gomez de Santos et al., 2021)).

The design of a reliable and accurate HTS assay is indispensable to identify mutants of interest in directed evolution campaigns. As witnessed by GC-MS, the cleavage of NNBT through the *N*-dealkylating activity of UPO releases a secondary aromatic amine and lactaldehyde, **Figure 3**. Thus, the latter was coupled to a colorimetric reporter (Purpald reagent, (Hopps, 2000)) in order to quantify the *N*-dealkylating activity of UPO in end-point mode. To validate the assay, the linearity and coefficient of variation (CV) was determined using fresh transformants from microtiter plate fermentations, **Figure 4**. First, we examined the relationship between the absorbance and UPO concentration. Transformants expressing the GroGu mutant were inoculated in a 96-well plate, and different volumes of the supernatants into which the UPO was secreted by yeast were assessed. When 40–100 μL of supernatant was used, a strong correlation was found between the amount of UPO secreted and

the absorbance at 530 nm, corresponding to the lactaldehyde released. To calculate the CV of the assay, one 96 well plate was inoculated with the parental GroGu in the different wells, fermented and assessed. The CV of the assay (19%) was a high but acceptable value to explore mutant libraries. Given the low initial activity of the GroGu mutant on NNBT, an improvement in the CV can be expected over the course of laboratory evolution, as happens when starting a directed evolution experiment with poor enzyme substrates.

The HTS assay was then used to evaluate a small subset of mutant libraries (200 clones each) constructed by error-prone PCR and *in vivo* shuffling, and using polymerases with different mutational bias (MnCl₂/Taq polymerase and mutazyme/GeneMorph II). To achieve a broader assessment of the assay, we introduced different mutational loads correlated with a set of mutagenic landscapes, **Figure 5**. The HTS method revealed that the *N*-dealkylation activity of UPO towards NNBT is susceptible to improvement by directed evolution. Given that several mutagenic conditions were applied, the mutant libraries presented different landscapes defined by the proportion of inactive clones, **Table 1** and **Figure 5**. This reflects the mutation rate since the frequency of deleterious mutations, negative epistasis and stop codons increases as more mutations are introduced. Accordingly, the most aggressive conditions of libraries 1 and 6 resulted in an excessive number of inactive clones, in contrast to the milder conditions of libraries 3, 4 and 5, the landscapes of which suggested that insufficient mutations were added. Commonly, an error rate around 40–50% in a mutant library is considered the standard to approach evolution by error-prone PCR (Salazar and Sun, 2003). Therefore, the conditions of library 2 or even library 7 may meet the requirements to carry out future directed evolution.

While the colorimetric assay along with the expression system presented in our study is useful to identify variants with improved *N*-dealkylation activity on surrogate NNBT, a detailed analysis of the reaction with real material becomes essential to provide insights on the degradation capacity of UPO mutants on epoxy resins (work ongoing). This set of experiments include techniques focus on determining the potential release of molecules to the reaction media (*e.g.,* by high performance liquid chromatography -HPLC-, turbidimetry, fluorimetry, UV/VIS spectroscopy) but also the analysis of the material after enzymatic treatment (*e.g.,* by differential scanning calorimetry -DSC-, thermal gravimetric analysis -TGA-, gel

TABLE 1 | Mutagenic conditions for the construction of mutant libraries.

Library	Polymerase	MnCl₂ Concentration [mM]	Number of Cycles	Inactive Clones (%)[a]
1	Taq polymerase	0.15	30	91
2	Taq polymerase	0.10	30	43
3	Taq polymerase	0.015	30	15
4	Taq polymerase	0.010	30	9
5	Taq polymerase	0.005	30	8
6	Mutazyme II	---	30	72
7	Mutazyme II	---	20	61

[a]Inactive clones are considered those with less than a 10% of the parental type activity.

permeation chromatography -GPC- or scanning electron microscopy -SEM-, among other techniques).

CONCLUSION

The present study set out the bases to address directed UPO evolution for epoxy resin biodegradation. Using a model compound that included the main features of the epoxy resin Hexflow® RTM6, a colorimetric HTS assay was developed and it was used to screen UPO mutant libraries constructed in and expressed by *S. cerevisiae*. This HTS assay could be helpful not only in the framework of a laboratory evolution workflow but also, as a general assay to detect *N*-dealkylation activity on biological samples. Given that activity improvements would be expected over the course of directed evolution, larger and more accurate model scaffolds could be synthesized and incorporated for study, thereby ensuring better focus on the whole polymer structure (work ongoing). For the practical treatment of epoxy resins, the engineering of both the enzyme and the process is paramount. In this regard, the use of organic solvents that help solubilize the recalcitrant material seems to be necessary to enhance availability for enzymatic attack. In this complex working scenario, new UPO variants are being developed with higher activity in non-conventional media and with broader specificities (Martin-Diaz et al., 2018; Gomez de Santos et al., 2021; Martin-Diaz et al., 2021). Along these lines, the use of chemical and mechanical pretreatment of resins, together with new resin formulations containing more attackable motifs, will complete the future developments aimed at enhancing the treatment of composites and managing their disposal.

REFERENCES

Acebo, C., Ramis, X., and Serra, A. (2017). Improved Epoxy Thermosets by the Use of Poly(ethyleneimine) Derivatives. *Phys. Sci. Rev.* 2 (8). doi:10.1515/psr-2016-0128

Alcalde, M. (2015). Engineering the Ligninolytic Enzyme Consortium. *Trends Biotechnol.* 33, 155–162. doi:10.1016/j.tibtech.2014.12.007

Beltran-Nogal, A., Sanchez-Moreno, I., Mendez-Sanchez, D., Gomez de Santos, P., Hollmann, F., and Alcalde, M. (2022). Surfing the Wave of Oxyfunctionalization Chemistry by Engineering Fungal Unspecific Peroxygenases. *Curr. Opin. Struct. Biol.* 73, 102342. doi:10.1016/j.sbi.2022.102342

Gharde, S., and Kandasubramanian, B. (2019). Mechanothermal and Chemical Recycling Methodologies for the Fibre Reinforced Plastic (FRP). *Environ. Tech. Innovation* 14, 100311. doi:10.1016/j.eti.2019.01.005

Gomez de Santos, P., Hoang, M. D., Kiebist, J., Kellner, H., Ullrich, R., Scheibner, K., et al. (2021). Functional Expression of Two Unusual Acidic Peroxygenases from *Candolleomyces Aberdarensis* in Yeasts by Adopting Evolved Secretion Mutations. *Appl. Environ. Microbiol.* 87, e00878. doi:10.1128/AEM.00878-21

Greene, J. P. (2021). "11–Thermoset Polymers," in *Automotive Plastics and Composites*. Editors J. P. Greene (William Andrew Publishing), 175–190. doi:10.1016/B978-0-12-818008-2.00002-7

Hofrichter, M., and Ullrich, R. (2014). Oxidations Catalyzed by Fungal Peroxygenases. *Curr. Opin. Chem. Biol.* 19, 116–125. doi:10.1016/j.cbpa.2014.01.015

Hopps, H. B. (2000). Purpald (R): a Reagent that Turns Aldehydes Purple. *Aldrichimica Acta* 33 (1), 28–30.

Hou, S., Hoyle, D. M., Blackwell, C. J., Haernvall, K., Perz, V., Guebitz, G. M., et al. (2016). Hydrolytic Degradation of ROMP Thermosetting Materials Catalysed by Bio-Derived Acids and Enzymes: from Networks to Linear Materials. *Green. Chem.* 18, 5190–5199. doi:10.1039/c6gc00378h

Lucas, N., Bienaime, C., Belloy, C., Queneudec, M., Silvestre, F., and Nava-Saucedo, J.-E. (2008). Polymer Biodegradation: Mechanisms and Estimation Techniques - A Review. *Chemosphere* 73, 429–442. doi:10.1016/j.chemosphere.2008.06.064

Martin-Diaz, J., Molina-Espeja, P., Hofrichter, M., Hollmann, F., and Alcalde, M. (2021). Directed Evolution of Unspecific Peroxygenase in Organic Solvents. *Biotechnol. Bioeng.* 118, 3002–3014. doi:10.1002/bit.27810

Martin-Diaz, J., Paret, C., García-Ruiz, E., Molina-Espeja, P., Alcalde, M., and Schottel, J. L. (2018). Shuffling the Neutral Drift of Unspecific Peroxygenase in *Saccharomyces cerevisiae*. *Appl. Environ. Microbiol.* 84, e00808. doi:10.1128/AEM.00808-18

Moeser, K. (2014). Enzymatic Degradation of Epoxy Resins: An Approach for the Recycling of Carbon Fiber Reinforced Polymers. *Amr* 1018, 131–136. doi:10.4028/www.scientific.net/amr.1018.131

Molina-Espeja, P., Garcia-Ruiz, E., Gonzalez-Perez, D., Ullrich, R., Hofrichter, M., and Alcalde, M. (2014). Directed Evolution of Unspecific Peroxygenase from *Agrocybe Aegerita*. *Appl. Environ. Microbiol.* 80, 3496–3507. doi:10.1128/aem.00490-14

Molina-Espeja, P., Ma, S., Mate, D. M., Ludwig, R., and Alcalde, M. (2015). Tandem-yeast Expression System for Engineering and Producing Unspecific Peroxygenase. *Enzyme Microb. Tech.* 73-74, 29–33. doi:10.1016/j.enzmictec.2015.03.004

Morelle, X., Lani, F., Melchior, M., André, S., Bailly, C., and Pardoen, T. (2012). "The Elasto-Viscoplasticity and Fracture Behaviour of the RTM6 Structural Epoxy and Impact on the Response of Woven Composites," in

DATA AVAILABILITY STATEMENT

The raw data supporting the conclusions of this article will be made available by the authors, without undue reservation.

AUTHOR CONTRIBUTIONS

MD, IM and JV-G carried out the experiments. DM-S carried out GC-MS experiments. IS-M and PG contributed to the design and implementation of the research. MD wrote the manuscript with support from JV-G and MA. MA and JV-G conceived the original idea and supervised the project.

FUNDING

15th European Conference On Composite Materials, Venice, Italy, June 24–28, 2012.

Morelle, X. (2015). Mechanical Characterization and Physics-Based Modeling of Highly-Crosslinked Epoxy Resin. Doctoral Thesis. Louvain, Belgium: Université catholique de Louvain. Institute of Mechanics, Materials and Civil Engineering.

Pickering, S. J. (2006). Recycling Technologies for Thermoset Composite Materials-Current Status. *Composites A: Appl. Sci. Manufacturing* 37, 1206–1215. doi:10.1016/j.compositesa.2005.05.030

Salazar, O., and Sun, L. (2003). Evaluating a Screen and Analysis of Mutant Libraries. *Methods Mol. Biol.* 230, 85–97. doi:10.1385/1-59259-396-8:85

Sauer, M., and Kuhnel, M. (2019). Composites Market Report 2019. Carbon Compos. Available at: https://composites-united.com/media/3988/eng_ccev_market-report_2019_short-version.pdf (September 2019), 1–11.

Zhang, Y., Zhang, L., Yang, G., Yao, Y., Wei, X., Pan, T., et al. (2021). Recent Advances in Recyclable Thermosets and Thermoset Composites Based on Covalent Adaptable Networks. *J. Mater. Sci. Tech.* 92, 75–87. doi:10.1016/j.jmst.2021.03.043